Large Area Silicon Nanomembrane Photonic Devices on Unconventional Substrates

Xiaochuan Xu, Harish Subbaraman, *Member, IEEE*, David Kwong, Amir Hosseini, Yang Zhang, and Ray T. Chen, *Fellow, IEEE*

***Abstract*— Silicon photonics on unconventional substrates have demonstrated great promise in tremendous unprecedented applications. One challenge is transferring high quality and large scale crystalline silicon nanomembranes onto various substrates. We developed a low temperature nanomembrane transfer technique based on adhesive bonding and deep reactive ion etching. A large area (2 cm × 2 cm), 250 nm thick silicon nanomembrane is defect-freely transferred onto a glass slide. The average propagation loss of a single mode waveguide (500 nm wide) fabricated on the transferred silicon nanomembrane is ∼4.3 dB/cm, which is comparable with those fabricated on silicon-on-insulator. To demonstrate the capability of accommodating large scale intricate photonic circuit, a 1 × 16 power splitter, consisting of photonic components with dimensions ranging from 119.4 μm to as small as 80 nm, is fabricated. An output uniformity of 0.96 dB at 1545.6 nm across all channels and an insertion loss of 0.56 dB are experimentally demonstrated.**

***Index Terms*— Optical waveguide, photonic integrated circuit, silicon nanomembrane, wafer bonding.**

I. Introduction

SILICON is not only the foundation of the microelectronics industry, but is also an appealing material for high density integrated photonics because of its high index and low cost mass production capabilities. It is a natural desire to replicate the success of silicon on different substrates and explore applications out of the scope of traditional silicon wafer based electronics and photonics [1]. One example is silicon planar lenses for visible wavelengths. Silicon has very high index but also strong absorption in visible wavelengths. However, the absorption loss of an ultrathin (<180 nm) crystalline silicon is negligible [2]. Thus, transferring silicon nanomembrane (SiNM) onto substrates transparent to visible wavelengths (e.g. glass) is of great importance in this research area. Another example is flexible silicon photonics. SiNMs exhibit excellent flexibility [1], which has rarely been noticed because of the rigid substrate. Transferring SiNMs onto flexible polyimide substrates can break the substrate limitations [3]. These interesting applications demand reliably transferring large scale crystalline SiNM, but current methods can only transfer small areas of SiNMs [1], [3]–[5], or a larger SiNM in the centimeter scale with meshed morphology [6], [7]. Photonic devices are too large compared to the transferrable area. Besides, photonic devices are extremely sensitive to geometry and defects, and thus the requirements for the feasibility of the transfer process is quite stringent. A few attempts have been reported [3], [8], but the transferrable area has remained limited. In this letter, we report a defect-free transfer of a large area (2 cm × 2 cm) of unpatterned SiNM onto a 1 mm thick glass substrate utilizing low temperature adhesive bonding [9] and deep reactive ion etching (DRIE). Unlike the transfer process described in [1], the SiNM has not been released from substrates during the transfer process. The processing temperature is kept $\leq$ 95 °C, so the technique can easily be applied to transfer SiNM onto other rigid and flexible substrates.

Manuscript received May 7, 2013; revised June 16, 2013; accepted June 30, 2013. Date of publication July 17, 2013; date of current version July 29, 2013. This work was supported in part by Air Force Office of Scientific Research STTR under Grant FA 9550-11-C-0014 monitored by Dr. G. Pomrenke.

X. Xu, D. Kwong, Y. Zhang, and R. T. Chen are with the University of Texas, Austin, TX 78758 USA (e-mail: xiaochuan.xu@utexas.edu; diddykwong@gmail.com; magicloudy@gmail.com; raychen@uts.cc.utexas.edu).

H. Subbaraman and A. Hosseini are with Omega Optics. Inc., Austin, TX 78759 USA (e-mail: harish.subbaraman@omegaoptics.com; amirh@utexas.edu).

Color versions of one or more of the figures in this letter are available online at http://ieeexplore.ieee.org.

Digital Object Identifier 10.1109/LPT.2013.2272678

II. Fabrication Process

The process flow is described in Fig. 1. The entire material stack from top-down contained a silicon-on-insulator (SOI) chip (including a 675 μm silicon handle, a 3 μm BOX layer, a 250 nm single crystal silicon device layer), a 5 μm SU-8 coated on the silicon device layer, a 5 μm SU-8 coated on the glass slide, and a 1 mm thick glass slide (Fig.1a). Before bonding, a 2 cm × 2 cm SOI chip and a 2.5 cm × 2.5 cm glass slide were thoroughly cleaned in piranha solution. The native oxide was removed with buffered oxide etchant (BOE). Both the chip and the slide were dehydrated in a convection oven. Next, a 5 μm thick SU-8 layer was spun on the SOI chip and the glass slide, and soft baked at 95 °C to evaporate the solvent. Then, the chip was put upside down on the glass slide and placed in an oven at 65 °C for 20 mins without applying pressure. The glass transition temperature of the non-cross-linked SU-8 is 64 °C [10], [11], and at the temperature or above, SU-8 exhibits excellent self-planarization, which minimizes the thickness variations [11]. Pressure was applied afterwards through a home-made bonder, which is shown in Fig. 1g. The material stack was mounted between the two thick Pyrex glass slides. The steel ball and the Belleville washer spread the point force generated by the thumb screw onto the thick Pyrex glass plate, forming a gradient pressure distribution. This pressure distribution avoided the formation

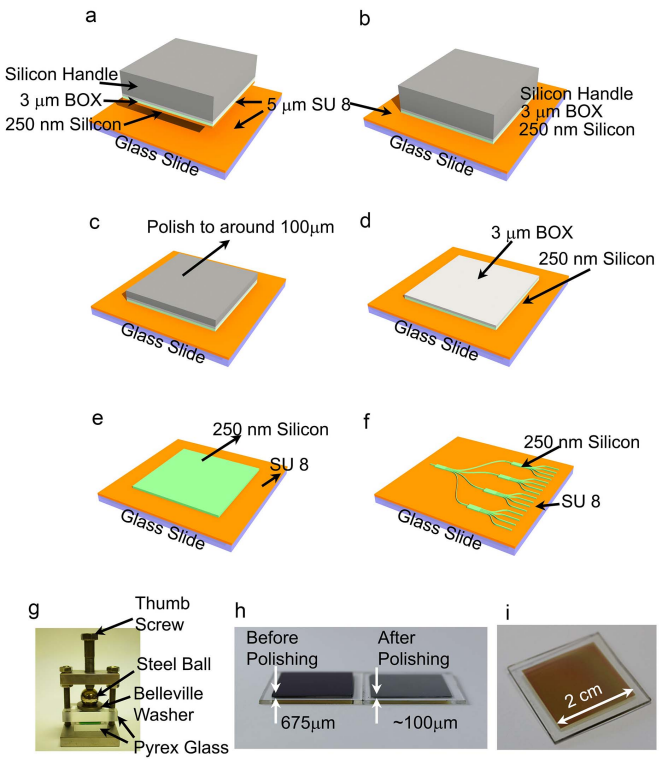

Fig. 1. Transfer process flow chart. (a). The material stack structure. (b). Bond the SOI chip upside down onto the glass slide. (c). Polish the silicon handle to $\sim$100 μm. (d). Etch the silicon handle away with DRIE. (e). Remove BOX with HF solution. (f). Pattern the transferred SiNM. (g). The home-made bonder. (h). Side view of a sample before and after polishing. (i). Transferred SiNM after removing the handle.

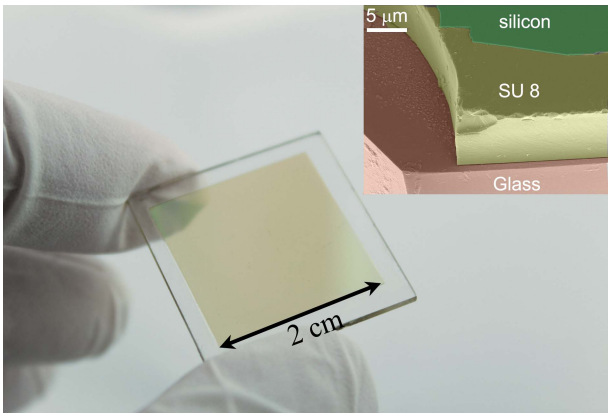

Fig. 2. Transferred SiNM on glass slide. Inset: tilted view of the transferred SiNM, showing the three layers: SiNM, SU-8, and glass. After transfer, the SU-8 layer is 9.4 m thick.

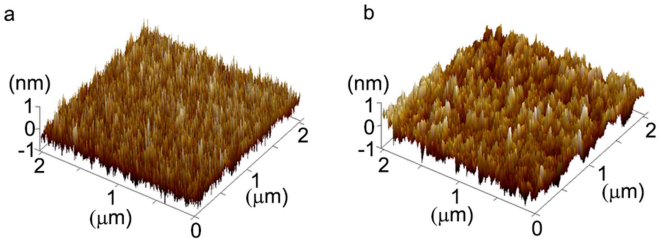

Fig. 3. Top surface roughness (a) before transfer and (b) after transfer.

of air cavities in between the two SU-8 layers. The thermal expansion of Belleville washers also compensated pressure decreasing induced by the reflow of the polymer. The sample was kept in a 65 °C vacuum oven for 20 hours to let polymer reflow and squeeze out the trapped air bubbles. After that, the sample was illuminated by 365 nm ultraviolet light through the glass slide to crosslink the SU-8 polymer. Exposure dose was around 150 mJ/cm^2. A long term post exposure bake (PEB) at 65 °C was done to further crosslink SU-8. Baking at a low temperature helped minimizing the strain, as the thermal expansion coefficients of silicon and SU-8 are different.

After bonding, the silicon handle was removed by DRIE, as described in Figs. 1c and 1d. Since DRIE generates tremendous heat, the carrier wafer was kept at $\sim$ 10 °C through Helium flow underneath. However, the thermal conductivities of SU-8 and glass slides were merely 0.2 W/mK and 0.96 W/mK, respectively, and thus the heat cannot be dissipated fast enough. Consequently, a significant temperature gradient built up between the top surface and the glass slide, subjecting the sample to cracking. The mismatch of the coefficients of thermal expansion (CTE) further aggravated the problem. To control the thermal budget, the silicon handle was mechanically polished down to $\sim$ 100 μm, as shown in Fig. 1c and Fig. 1h, to shorten the etching time. The etching recipe was also carefully modified. The inductively coupled plasma (ICP) power was tuned to keep it slightly above the threshold of maintaining plasma to reduce the heat generation rate to match the heat dissipation rate. The silicon etch rate of this recipe was around 2.7 μm/cycle, with selectivity $\sim$80 of oxide to silicon. The 3 μm BOX was used as a stopping layer to protect the SiNM underneath, and it could be removed by hydrofluoric (HF) acid etching afterwards. The SiNM after DRIE is shown in Fig. 1i.

Before removing the BOX layer, photoresist was applied on both the bottom and the top of the sample except the BOX region. Instead of immersing the whole sample into HF solution, which could cause delamination, a few droplets of HF were applied on the BOX directly. The surface tension of the silicon dioxide constrained the solution within the SiNM without flowing over. A picture of the transferred SiNM is shown in Fig. 2. After transfer, the thickness of the SU-8 was measured to be around 9.4 μm. The transferred SiNM was examined with an optical microscope, and no visible defects were identified. The transferred SiNM can be patterned into photonic structures through conventional techniques such as photolithography and electron beam lithography, as shown in Fig. 1f. The latter was used in this letter. The patterning process was similar to that described in [12].

III. Characterization

A. Surface Roughness and Strain

To investigate the quality of the transferred SiNM, the top surface roughness of SiNMs before and after transfer was measured through atomic force microscopy (AFM). An increasing of roughness has been observed, as shown in Fig. 3a and b.

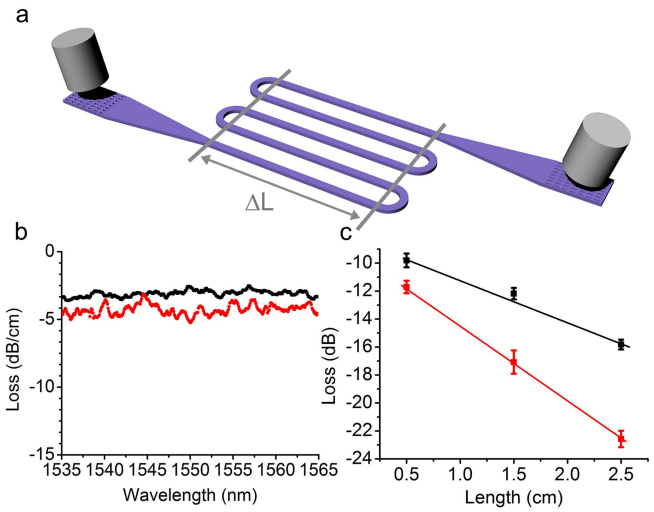

Fig. 4. (a). Schematic of the loss measurement structure. Different propagation length is obtained through varying Δ L. (b). The propagation loss of single mode waveguides on the transferred SiNM (red) and on SOI (black). (c). The slope loss at 1550 nm.

The surface roughness of the transferred SiNM was 0.522 nm, while it was 0.128 nm for SOI. Energy dispersion spectrometry showed rich carbon, hydrogen, and oxygen elements in the white spots in the AFM images indicating that these spots were possibly the polymer residues from the DRIE process. Since the ICP power was kept low, the polymer deposited in the deposition step cannot be stripped completely during the silicon etching step and deposit on the nanomembrane during the processes followed. However, the polymer spots were small so that the effects on propagation loss were limited. Attempts also have been made to measure the stress of the nanomembrane through Raman scattering, but the wavelength shift was not detectable, indicating the strain was less than 10 MPa (detect limitation of the machine).

B. Propagation Loss

Since propagation loss is a deterministic factor to investigate whether a material is suitable for photonic applications, the cut-back method is used to measure the propagation loss of single mode waveguides fabricated on transferred SiNMs. To determine the propagation loss, 500 nm wide single mode waveguides with different lengths are fabricated. The schematic of the testing structure is shown in Fig. 4a. SWG couplers described in [12] and [13] are utilized for input and output light coupling. 10 μm wide, 17 μm long SWG couplers are connected to the single mode waveguide through a 500 μm adiabatic taper. Through varying ΔL, different length of single mode waveguide (0.5 cm, 1.5 cm, and 2.5 cm) can be constructed. A set up described in [12] is exploited for measurements. Light from a broadband amplified spontaneous emission (ASE) light source is transverse-electric (TE) polarized and coupled into the single-mode waveguide via a 10^{o} tilted polarization maintaining fiber. The output light is collected by a single mode fiber tilted at the same angle as the input fiber, and analyzed in an optical spectrum analyzer.

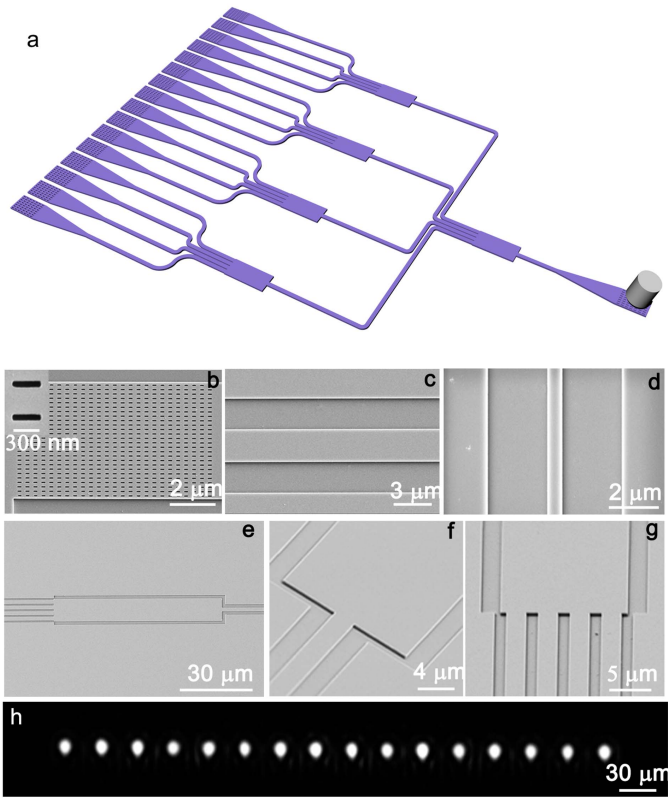

Fig. 5. (a) Schematic of the 1 × 16 optical power splitter composed of two-level cascaded 1 × 16 MMIs. SEM picture of (b) the subwavelength grating coupler for in and output coupling, (c) the 2 μm wide multimode waveguide, (d) 500 nm single mode waveguide, (e) the 1 × 4 MMI, (f) the access waveguide of the 1 × 4 MMI, (g) and the output waveguides of the 1 × 4 MMI, (h) the infrared image of the sixteen output spots captured with a 45° tilted camera.

The results are presented in Fig. 4b and c. The average propagation loss is about 4.3 dB/cm in the wavelength range from 1535 nm to 1565 nm for waveguides fabricated on transferred SiNMs, while the value is around 3.1 dB/cm for SOI based single mode waveguides with the same dimensions. The increment of the propagation loss matches the observations of the roughness increasing.

C. Demonstration of Patterning Intricate Photonic Devices

To demonstrate the feasibility of fabricating photonic devices with intricate structures on the transferred SiNM, a 1 × 16 splitter, formed by cascading five 1 × 4 MMIs together, is designed for air (top) and SU-8 (bottom) cladding. A schematic of the optical splitter is provided in Fig. 5a. The length and width of the multimode regions are 119.4 μm and 16 μm, respectively. The air holes of the subwavelengths structure is 80 × 345 nm The input and access waveguides are both 2.5 μm wide to ensure low insertion loss and high uniformity [14]. Subwavelength grating couplers are again used for input and output light coupling. Figs. 5b ∼g show the details of each section of the splitter. To clearly resolve the individual output spots using a 45° tilted infrared camera, a fanout design is used to separate the 16 MMI output channels by 30 μm. A tunable laser with a wavelength precision of

0.001 nm is exploited to scan the working wavelength of the splitter. Fig. 5h shows the infrared image of the 16 output spots. A uniformity of 0.96 dB is obtained at 1545.60 nm across the 16 output channels, while the insertion loss for the device is 0.56 dB. The uniformity and the insertion loss are determined by using a single mode fibre to scan the output power of each output channel. The performance is quite acceptable and is comparable with SOI based MMI splitters [14].

IV. Conclusion

We develop a low temperature transferring technique based on adhesive bonding and deep silicon etching, with which 2 cm $\times$ 2 cm large, 250 nm thick SiNMs are transferred successfully. The loss of the 500 nm wide single mode waveguide fabricated on the transferred SiNM is 4.3 dB/cm, which is comparable with those fabricated on the SOI. A 1 $\times$ 16 splitter, consisting of two cascaded levels of 1 $\times$ 4 MMIs, is fabricated. The testing results show high uniformity of 0.96 dB, and a low insertion loss of 0.56 dB. This method can be applied to transfer SiNM onto substrates other than glass. It will extend the application scale of silicon photonics.

References

[1] J. A. Rogers, M. G. Lagally, and R. G. Nuzzo, "Synthesis, assembly and applications of semiconductor nanomembranes," *Nature*, vol. 477, no. 7362, pp. 45–53, 2011.

[2] Z. Peng, D. A. Fattal, A. Faraon, M. Fiorentino, J. J. Li, and R. G. Beausoleil, "Reflective silicon binary diffraction grating for visible wavelengths," *Opt. Lett.*, vol. 36, no. 8, pp. 1515–1517, 2011.

[3] X. C. Xu, H. Subbaraman, A. Hosseini, C. Y. Lin, D. Kwong, and R. T. Chen, "Stamp printing of silicon-nanomembrane-based photonic devices onto flexible substrates with a suspended configuration," *Opt. Lett.*, vol. 37, no. 6, pp. 1020–1022, 2012.

[4] D. H. Kim, *et al.*, "Epidermal electronics," *Science*, vol. 333, no. 6044, pp. 838–843, 2011.

[5] D. H. Kim, *et al.*, "Stretchable and foldable silicon integrated circuits," *Science*, vol. 320, no. 5875, pp. 507–511, 2008.

[6] Y. Yang, *et al.*, "Arrays of silicon micro/nanostructures formed in suspended configurations for deterministic assembly using flat and roller-type stamps," *Small*, vol. 7, no. 4, pp. 484–491, 2011.

[7] J. H. Seo, *et al.*, "'Large-area printed broadband membrane reflectors by laser interference lithography," *IEEE Photon. J.*, vol. 5, no. 1, p. 2200106, Feb. 2013.

[8] M. J. Zablocki, A. Sharkawy, O. Ebil, and D. W. Prather, "Nanomembrane transfer process for intricate photonic device applications," *Opt. Lett.*, vol. 36, no. 1, pp. 58–60, 2011.

[9] F. Niklaus, G. Stemme, J. Q. Lu, and R. J. Gutmann, "Adhesive wafer bonding," *J. Appl. Phys.*, vol. 99, no. 3, pp. 031101-1–031101-28, 2006.

[10] K. Pfeiffer, M. Fink, G. Gruetzner, G. Bleidiessel, H. Schulz, and H. Scheer, "Multistep profiles by mix and match of nanoimprint and UV lithography," *Microelectron. Eng.*, vols. 57–58, pp. 381–387, Sep. 2001.

[11] T. Santeri and F. Sami, "Wafer-level bonding of MEMS structures with SU-8 epoxy photoresist," *Phys. Scripta*, vol. 2004, no. T114, p. 223, 2004.

[12] X. Xu, H. Subbaraman, J. Covey, D. Kwong, A. Hosseini, and R. T. Chen, "Complementary metal–oxide–semiconductor compatible high efficiency subwavelength grating couplers for silicon integrated photonics," *Appl. Phys. Lett.*, vol. 101, no. 3, pp. 031109–031104, 2012.

[13] H. Subbaraman, X. Xu, J. Covey, and R. T. Chen, "Efficient light coupling into in-plane semiconductor nanomembrane photonic devices utilizing a sub-wavelength grating coupler," *Opt. Express*, vol. 20, no. 18, pp. 20659–20665, 2012.

[14] A. Hosseini, H. Subbaraman, D. Kwong, Y. Zhang, and R. T. Chen, "Optimum access waveguide width for 1 $\times$ N multimode interference couplers on silicon nanomembrane," *Opt. Lett.*, vol. 35, no. 17, pp. 2864–2866, 2010.